AAS 25-160

RECOVERY FROM MISSED THRUST DURING GATEWAY'S NRHO INSERTION USING AUXILIARY PROPULSION

Scott N. Karn,[*] Steven L. McCarty,[†] and Melissa L. McGuire[‡]

Results are presented by which a high thrust reaction control system (RCS) can be used to complete insertion of the Gateway into a Near Rectilinear Halo Orbit (NRHO) in the event of a missed thrust event (MTE). Recovery solutions are presented in terms of the response time afforded, the Δv required, and the NRHO insertion delay relative to the reference trajectory. Results are presented for methodologies that maintain the reference trajectory NRHO insertion epoch as well as those that optimize this insertion epoch in order to buy down recovery costs and increase the robustness of solutions. This analysis presents solutions which, in the event of an MTE during NRHO insertion, enable RCS recoveries that require under 20 m/s Δv and less than four days of NRHO insertion delay.

INTRODUCTION

NASA's Artemis program, with the assistance of international and commercial partners, aims to return humanity to the lunar surface and establish a sustained human presence in cislunar space. To facilitate this goal, an orbital platform known as the Gateway will be placed in lunar orbit to facilitate the development, aggregation, and operation of critical mission infrastructure. The Gateway will be placed in a 9:2 resonant, Earth-Moon L2 Southern (L2S) Near Rectilinear Halo Orbit[1], referred to in this paper as the NRHO.

While the station will be built up over time with multiple modules supplied from various vendors, the initial capability of Gateway will be comprised of a Power and Propulsion Element (PPE) and a Habitation and Logistics Outpost (HALO). These two elements will be integrated together on the ground, then launched as a single stack to a highly elliptical Earth parking orbit. The combined Gateway vehicle will then transit to the NRHO along a low-thrust spiral trajectory, a description of which has been published previously[2]. The highly capable 50 kW class solar electric propulsion (SEP) system[3] onboard the PPE will be used to execute this Lunar Transit trajectory.

Previous work has described a methodology by which Gateway can recover from missed thrust events (MTEs) during low-thrust insertion into the NRHO using the SEP system[4]. These results show that, as designed, the Insertion Phase of the Lunar Transit trajectory is robust to MTEs during any of the deterministic thrust arcs, provided that the SEP system is operable one revolution

[*]Mission Design Engineer, Mission Architecture and Analysis Branch, NASA Glenn Research Center, 21000 Brookpark Road, Cleveland, OH, 44135
[†]Mission Design Engineer, Mission Architecture and Analysis Branch, NASA Glenn Research Center, 21000 Brookpark Road, Cleveland, OH, 44135
‡Power and Propulsion Element Mission Design Manager, Mission Architecture and Analysis Branch, NASA Glenn Research Center, 21000 Brookpark Road, Cleveland, OH, 44135

following an MTE. The work presented in this paper will focus on the use of the high-thrust reaction control system (RCS) to recover from MTEs during the Insertion Phase, the Δv costs associated with these strategies, and the response and recovery times that are required by mission operators.

BACKGROUND

Lunar Transit Reference Trajectory

Previously published work[4] described the design of reference Insertion Phase trajectories by which the Gateway may be delivered to the NRHO. This design methodology assumes five targeted perilune passes which are used to align the Gateway's trajectory with an optimal insertion into the NRHO. The first two of these revolutions are entirely ballistic, while the subsequent three each contain a single deterministic low-thrust maneuver culminating in a rendezvous with the reference NRHO. As the Gateway is targetting a pre-computed reference NRHO trajectory (with a specific phase)[1], insertion into this reference orbit must be executed as if Gateway is conducting a rendezvous with an in-situ spacecraft. This insertion geometry is depicted in **Figure 1**.

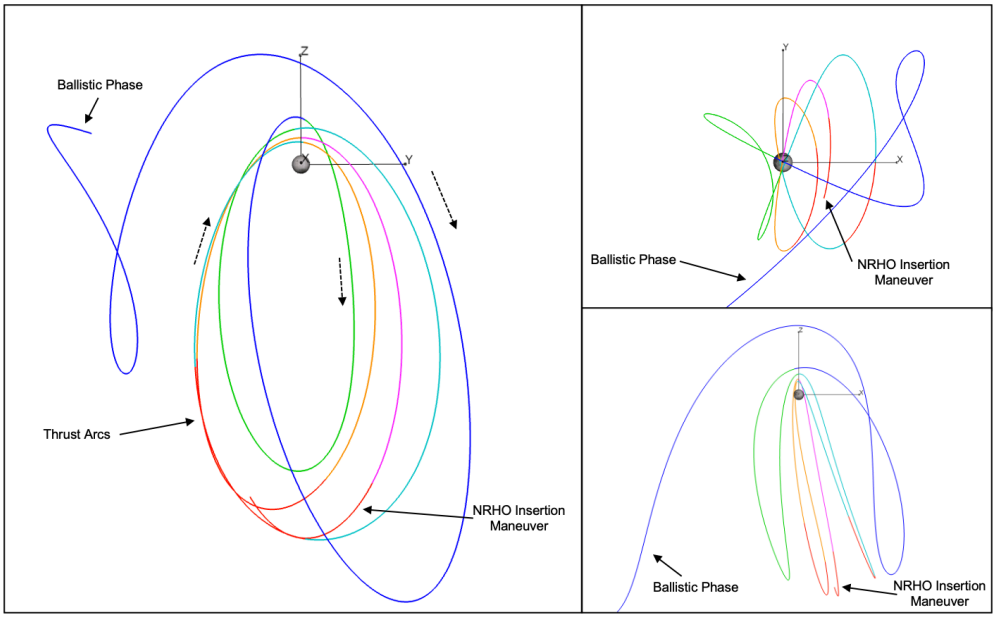

Figure 1: Three-axis view of the Lunar Transit Insertion Phase shown in the Earth-Moon rotating frame. The trajectory is colored by revolution (blue, then green, cyan, orange, and magenta) while thrust arcs are shown in red. The counterclockwise direction of motion is noted with dotted arrows

The deterministic Δv required to execute this Insertion Phase is dependent upon a number of factors, particularly the orientation of the initial Earth parking orbit and the Sun-Earth-Moon geometry at the time of insertion into the NRHO. With optimal alignment of the initial parking orbit (and the subsequent evolution of the trajectory) and a favorable orientation of the Sun-Earth-Moon system, Insertion Phase execution costs can be as low as 5 m/s Δv. These conditions are not always executable, however, and suboptimal parking orbit geometries must often be chosen in order to satisfy spacecraft and mission constraints and requirements. In these cases, execution of the Insertion Phase can be up to 100 m/s Δv, with a mean value across a 12-month span of launch opportunities of 22.65 m/s (**Figure 2**). This range of values is equivalent to between 0.3% and 3% of the total Δv required to execute the Lunar Transit in its entirety.

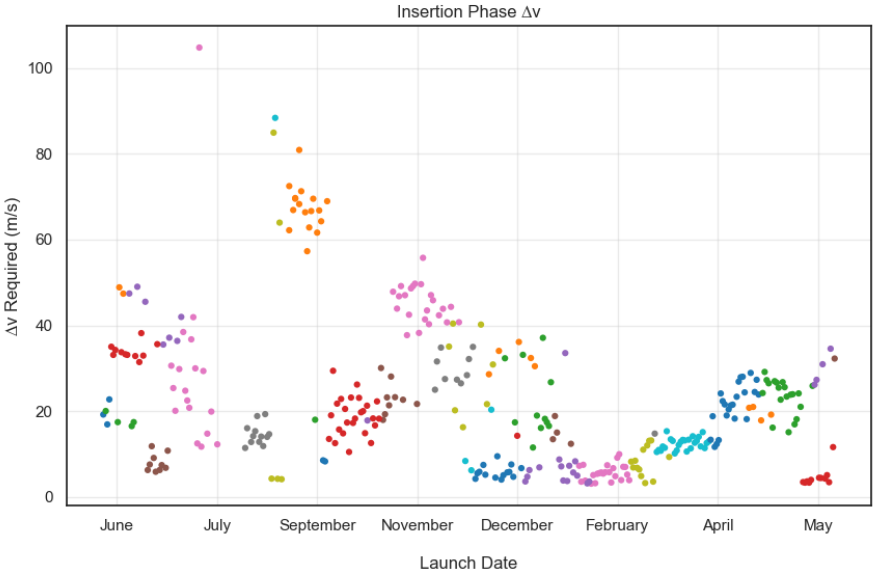

Figure 2: Insertion Phase Δv costs across one-year of launch dates. Solutions are colored by the apolune at which they arrive to the NRHO (solutions within the same color family arrive to the NRHO at the same apolune passage)

Missed Thrust

Missed thrust is a persistent threat to any low-thrust trajectory[6,7], the Lunar Transit being no exception. Broadly, a Missed Thrust Event (MTE) is defined as any time where the spacecraft cannot fully execute a planned low-thrust maneuver. Any number of spacecraft faults or anomalies may cause the vehicle to enter a safe mode or result in a ground commanded abort of a maneuver.

Following such an event, mission controllers and engineering teams will require some non-zero period of time to review telemetry, diagnose and address any vehicle faults, and determine whether it is safe to resume operation of the propulsion system. Recovery from an MTE thus cannot begin immediately following an event. Some amount of ground response time must be allowed before a recovery maneuver can be commanded. Previous analysis[4] assumed that thruster operations could not be resumed for one complete revolution, or roughly six days. As this work will consider the use of the chemical RCS, shorter response times are considered which would enable execution of recovery strategies beginning within one day of the planned low-thrust maneuver execution epoch.

METHODOLOGY

All trajectory design and optimization activities for this analysis are completed utilizing Copernicus[8], a trajectory design tool developed and managed at NASA's Johnson Space Center. The Sparse Nonlinear Optimizer (SNOPT)[9] is used for trajectory optimization. A monotonic basin hopping algorithm is also used as a wrapper around Copernicus to aid optimization[10]. The full-fidelity set of reference trajectory solutions discussed in **Figure 2** forms the basis for this work.

High Thrust Recovery

The RCS onboard the PPE is a high-thrust auxiliary propulsion system. As such, maneuvers executed with this system can be modeled as impulsive burns. This is in contrast to the nominal low-thrust maneuvers, which must be modeled as finite thrust arcs and can be several days in duration. It is common practice to first model a trajectory assuming impulsive maneuvers, then to convert those impulses to equivalent finite maneuvers once a converged solution is found. In the case of this analysis, the exact opposite will be done. A converged trajectory has already been computed with finite low-thrust maneuvers and an effort will be made to effectively replace those finite maneuvers with an equivalent impulse.

Replacing a deterministic finite maneuver with an impulsive burn is a typically a straightforward process, particularly when the analysis is enabled by an optimizer such as SNOPT. In the context of the Lunar Transit Insertion Phase, the exception to this is the NRHO Insertion Maneuver (NIM), where the Gateway will rendezvous with the NRHO reference trajectory at the end of the low-thrust maneuver. For this maneuver, the single deterministic thrust arc must be replaced with two impulsive burns, one to intercept the NRHO in position and a second to match the NRHO in velocity. The most simple implementation of this finite-to-impulsive conversion would be to place one burn at the epoch at which the low-thrust maneuver begins, and the other at the epoch at which the low-thrust maneuver ends. This is shown in **Figure 3**, which depicts the final revolution of the Insertion Phase and the NIM constructed with both a finite and impulsive maneuvers.

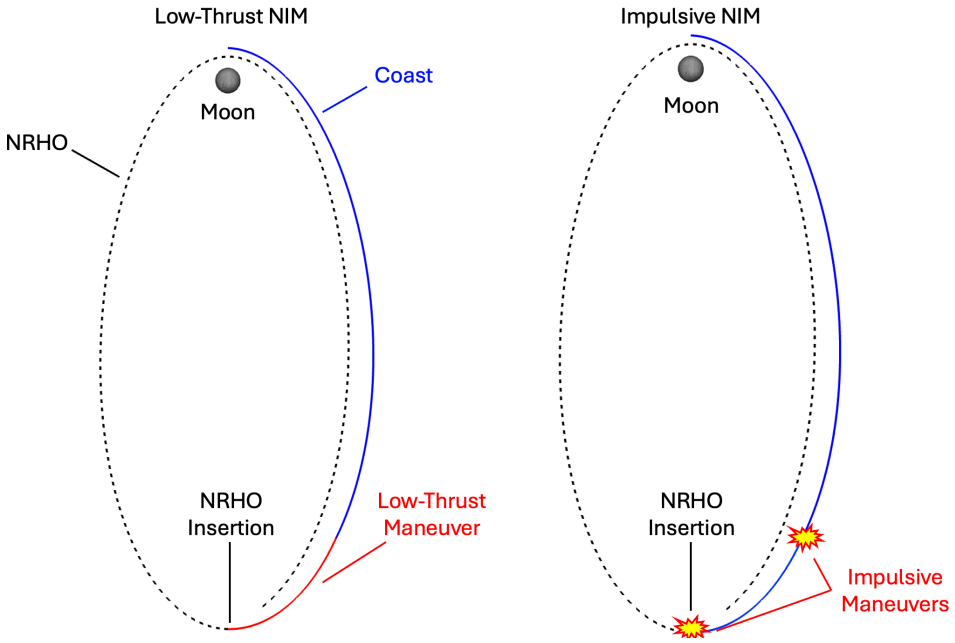

Figure 3: Notional depiction of the NRHO Insertion Maneuver when constructed with a low-thrust maneuver (left) and two impulsive burns (right)

This impulsive construction methodology presents challenges to a missed thrust recovery scenario. Locating the first burn to occur at the same epoch as the nominal insertion thrust arc means that the nominal as well as the recovery maneuvers would need to be commanded simultaneously. In the event of an MTE during the baseline NIM, some amount of time would be

necessary to determine the health of the spacecraft, develop or decide upon a recovery plan, then execute that recovery. Thus, the epoch of the first impulse must be constrained to occur after the start time of the nominal low-thrust maneuver. The costs associated with this execution delay are critical to understanding the maximum response time available to mission operators. To determine the magnitude of the maneuver required for a given execution delay, the time between the start of the nominal low-thrust maneuver and the execution of the first impulse is varied. This is depicted in **Figure 4**. For each execution delay case, the trajectory targets the reference NRHO at the conclusion of the second impulse.

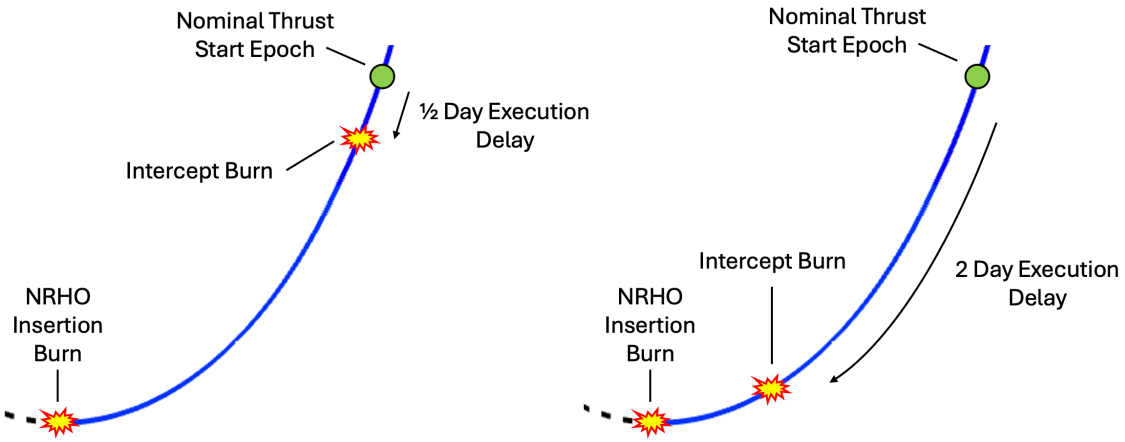

Figure 4: Impulsive insertion to the NRHO showing a 0.5 day intercept burn execution delay (left) and a 2-day intercept burn execution delay relative to the epoch at which the nominal low-thrust insertion maneuver begins (depicted with a green dot)

This paper will cover two specific analyses based upon the above methodology. In the first, arrival to the NRHO is fixed at the same epoch as the nominal Insertion Phase. In the second analysis, the NRHO insertion epoch is allowed to vary in order to maximize final mass (and thus minimize Δv). For these cases, the NRHO insertion epoch is allowed to float by up to three days later in time, which restricts NRHO insertion to occurring prior to perilune passage.

Methodology Scope

The presented methodologies do not represent an exhaustive or complete list of MTE recovery solutions available to Gateway during the Insertion Phase. The strategies presented are meant to serve as representative solutions that will form a basis for future maturation of a Lunar Transit missed thrust recovery strategy. Additionally, all analyses assume a complete failure to execute any portion of a planned maneuver, partial executions are not considered.

RESULTS

Execution Delay – Fixed Arrival Epoch

Critical to understanding the amount of ground response time available to operators in the event of an MTE during NRHO insertion is the Δv cost associated with a given execution delay. **Figure 5** shows the relationship of required Δv relative to execution delay for a single NRHO insertion maneuver during a single Lunar Transit trajectory (one of the 346 trajectories presented in **Figure 2**). In **Figure 5**, the total Δv required to complete NRHO insertion (shown in green) is further broken down into the Δv required to execute the intercept burn (blue) and the rendezvous burn

(orange). At an execution delay of zero, the intercept burn is executed at the same epoch as the start of the nominal low-thrust insertion maneuver and the total Δv required is evenly split between the intercept and rendezvous burns. With increasing execution delays, the split of Δv between the two impulsive burns becomes more and more uneven. The magnitude of the intercept burn grows with execution delay while the magnitude of the rendezvous burn reduces by nearly the same amount, resulting in a period of roughly flat insertion costs. This behavior is steady until a sharp inflection point (occurring at an execution delay of roughly 0.4 days in **Figure 5**), after which point the costs of both burns increase rapidly as the execution delay approaches an infeasible solution.

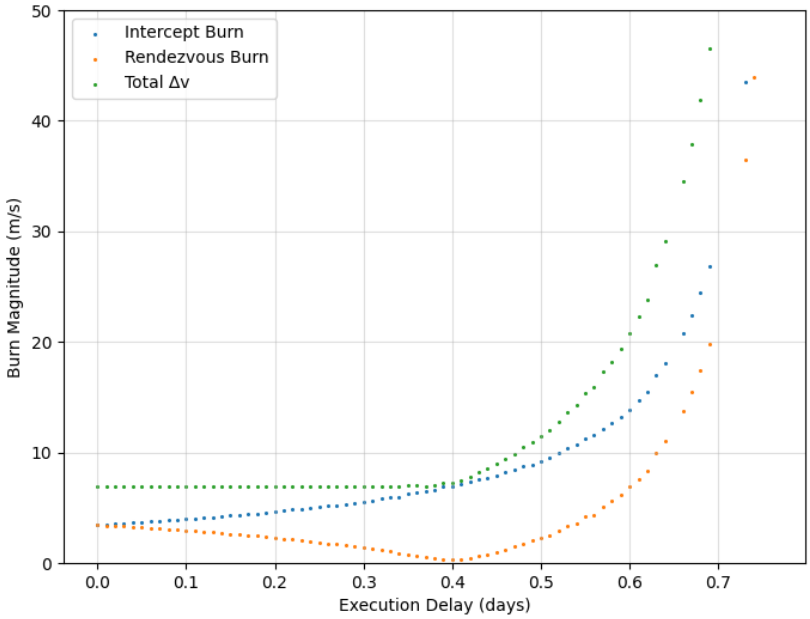

Figure 5: Required Δv as a function of execution delay for a single NRHO insertion. Results are broken down by intercept burn magnitude (blue), rendezvous burn magnitude (orange), and total Δv expended (green)

This inflection point clearly splits the solution space into two phases, one where insertion costs remain relatively flat and one where insertion costs rapidly rise and the magnitude of Δv required to complete NRHO insertion quickly makes recoveries for these execution delays infeasible to execute. **Figure 6** shows that this inflection point occurs at the time of closest approach (TCA) of the spacecraft trajectory relative to the NRHO. Due to the low control authority afforded by the SEP system, the Insertion Phase is designed to intercept the NRHO on the final revolution, with the final NRHO insertion maneuver completing the rendezvous with the target. Because of this, every reference trajectory's Insertion Phase experiences this same TCA behavior (which roughly coincides with the epoch of NRHO insertion of the nominal low-thrust insertion maneuver). As the execution delay approaches the TCA, the magnitude of the intercept burn grows while the magnitude of the rendezvous burn shrinks. If the execution of the intercept burn occurs directly at TCA, the intercept burn completes nearly all of the Δv required to insert into the NRHO with the rendezvous burn effectively serving as a trajectory correction maneuver (TCM) or clean-up burn. Execution delays that place the intercept burn after TCA result in increasing insertion costs as the spacecraft must correct the trajectory back towards the NRHO and insert as opposed to adjusting a trajectory that is already coasting towards the NRHO.

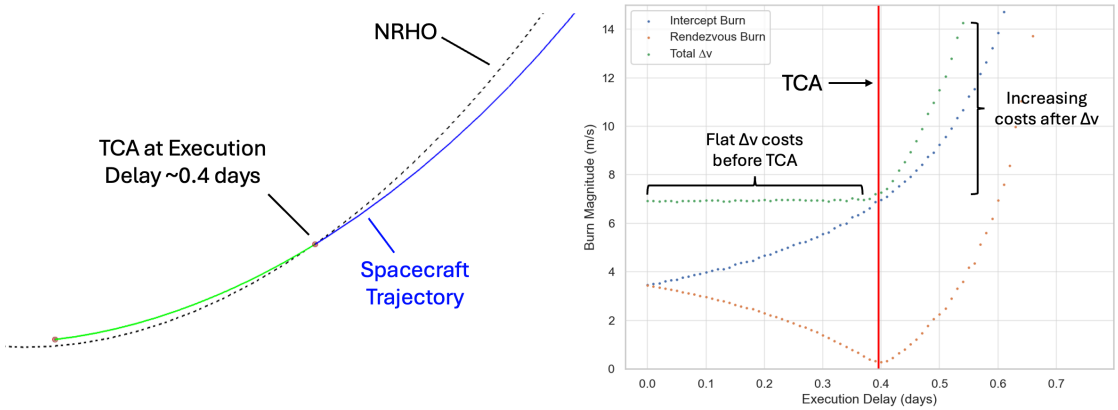

Figure 6: Time of Closest Approach (TCA) behavior (left) relative to Δv costs for impulsive insertion to the NRHO (right). Insertion Δv costs rise sharply after TCA, noted as a red vertical line on the left plot

This same TCA-dependent behavior is consistent across the entire solution space and is present in all reference trajectories. Furthermore, the exact trends of a specific solution set are dependent on the respective nominal Insertion Phase reference trajectory. This is seen clearly in **Figure 7**, which shows that the NRHO apolune passage at which an insertion occurs governs the behavior of the recovery solutions. Apolune passages are numbered sequentially, meaning that apolune #37 is the 37th NRHO apolune passage to occur in a given calendar year.

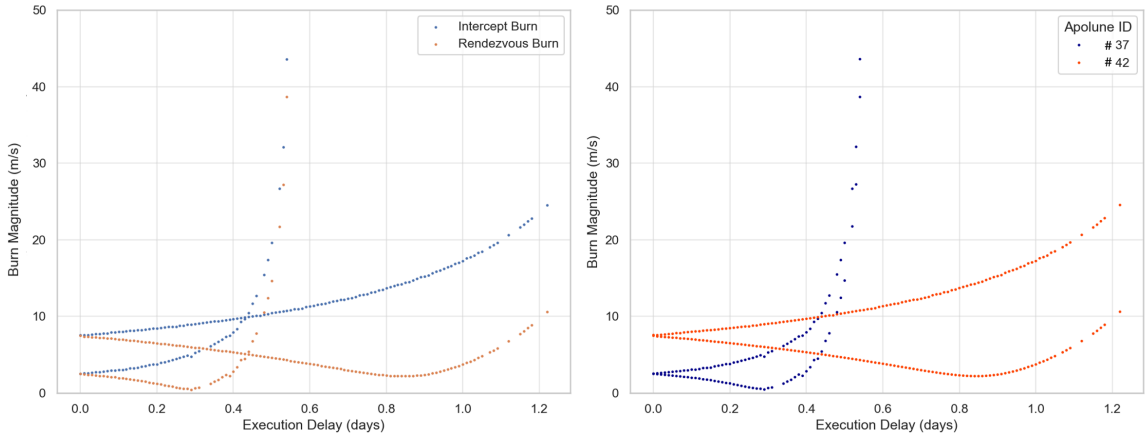

Figure 7: Intercept vs rendezvous burn behavior for two separate solutions. Magnitudes for each burn type are depicted on the left, while the figure on the right shows behavior dependency to the NRHO apolune at which insertion occurs

The sensitivity of a particular NRHO insertion maneuver to execution delays can be presented in terms of the additional Δv above nominal required to execute a particular impulsive insertion. As discussed above, the amount of execution delay that can be accomodated without increasing Δv costs is largely dependent upon the time between the start of the nominal low-thrust insertion maneuver and the TCA of the spacecraft with respect to the NRHO. This, in itself, is a function of the duration of the low-thrust maneuver, which is directly proportional to the magnitude of the nominal insertion maneuver. The dependency between Δv penalty as a function of execution delay and the magnitude of the nominal insertion is clearly shown in **Figure 8**, where larger nominal insertions (up to 25-30 m/s) enable longer execution delays without significant Δv penalties. This

contrasts with solutions that have smaller nominal insertions (near 5 m/s), which increase rapidly in Δv penalty as the execution delay grows beyond 0.25 days.

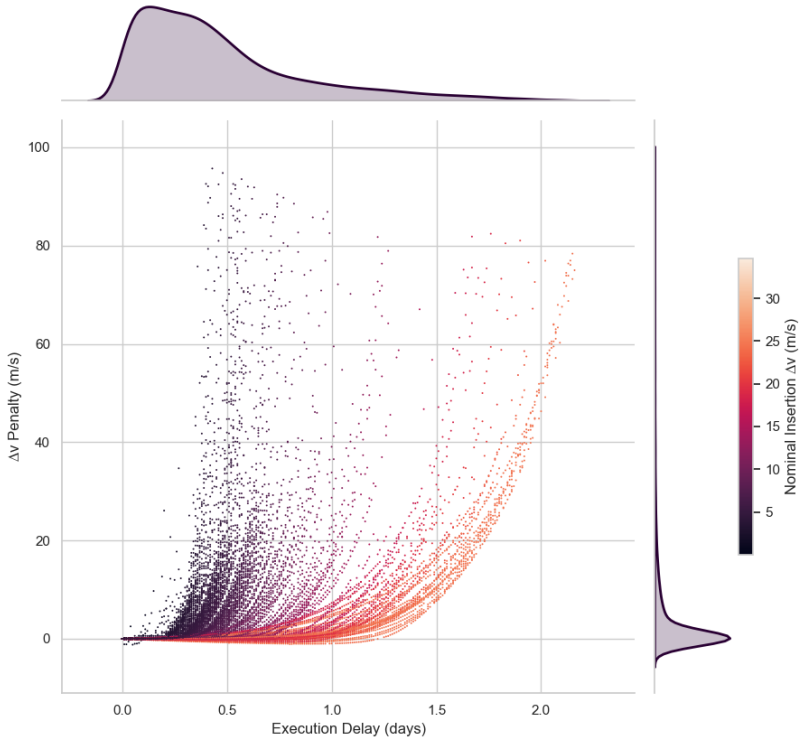

Figure 8: NRHO insertion Δv penalty as a function of execution delay colored by magnitude of the nominal insertion. The distribution of data across each axis is shown in the additional plots in the margins

The behavior shown in **Figure 8** clearly suggests a counterintuitive result, where the NRHO insertions which are most robust to MTEs and offer the most amount of recovery time without incurring a Δv penalty are the most expensive nominal insertions. Conversely, nominal NRHO insertions that require the lowest amount of propulsive Δv are the least robust to MTEs. This is shown in **Figure 9**, where the maximum possible execution delay can be seen based on the maginitude of the nominal NRHO insertion maneuver (execution delays beyond this maximum value result in infeasible solutions). From **Figure 9**, it can be seen that nominal insertion maneuvers of less than 10 m/s enable maximum execution delays of up to only one day. A high density of solutions can be seen between 3 and 7 m/s, which correspond to maximum execution delays of 0.4-0.75 days. Comparatively, a sparse number of solutions exist above 15 m/s where possible execution delays extend beyond 1.5 days. This is due to the construction of the nominal reference trajectories, which aims to maximize final mass delivered (and thus minimize expended propellant). Optimal solutions, and thus those that will be found by Copernicus, will be those that result in the minimum Δv required to complete the Lunar Transit. The result of this optimization is that the highest density of NRHO insertion maneuvers occur near 5 m/s Δv and offer less than 12 hours of ground response time before MTE recovery Δv penalties grow beyond 50 m/s. This short time frame means that for many of the solutions presented, a sufficient amount of time for operators to verify vehicle health, plan a recovery, then execute an intercept and rendezvous burn likely does not exist before the vehicle misses the planned NRHO insertion epoch.

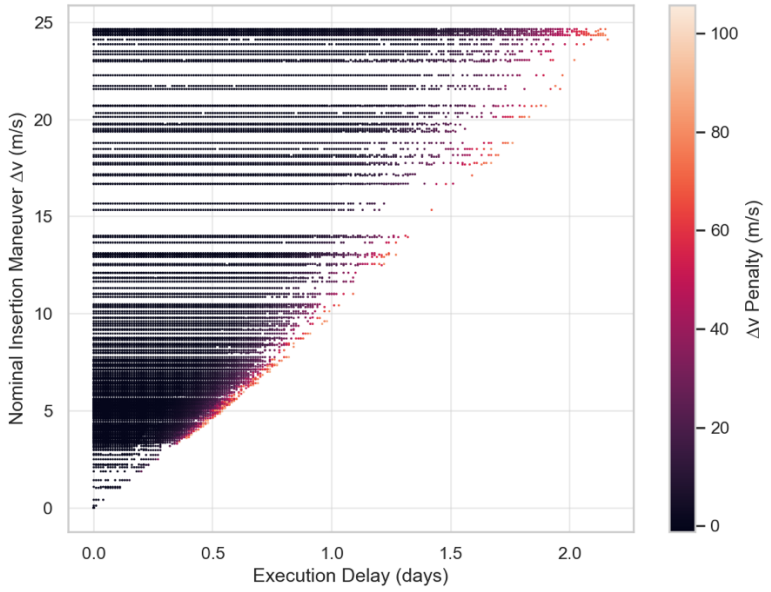

Figure 9: Maximum execution delay available as a function of nominal insertion maneuver Δv, colored by the Δv penalty associated with a given delay

Execution Delay – Variable Arrival Epoch

As discussed previously, maintaining a fixed NRHO insertion epoch results in a maximum execution delay that is slightly shorter than the duration of the nominal insertion maneuver. This means that the shortest nominal maneuvers, and thus the cheapest, are the least robust and afford the least amount of ground response time in the event of an MTE. It is, of course, desirable to find a way to make every solution in the reference trajectory set robust to MTEs.

This is accomplished by allowing the epoch of insertion into the NRHO to optimize in order to maximize mass delivered to the NRHO. This will result in a delayed arrival to the NRHO relative to the reference trajectory, but this also enables longer duration recovery solutions. Enabling a late arrival to the NRHO enables execution delays beyond the duration of the nominal low-thrust NRHO insertion maneuver and enables robust recovery solutions for short duration nominal insertions.

Figure 10 shows the number of feasible solutions for a fixed NRHO arrival epoch as a function of execution delay. While there are 346 total reference trajectories, the number of available recovery solutions quickly drops off as execution delay increases. In particular, this shows the number of reference trajectories with low-thrust insertion maneuvers shorter than 0.75 days as less than 100 recovery solutions exist that can accommodate an execution delay of at least 18 hours. Additionally, roughly 50 solutions (14.5% of the total number of reference trajectories) exist for an execution delay of 24 hours. **Figure 10** additionally shows that, by allowing the NRHO arrival epoch to optimize, 100% of the solution space can be recovered and execution delays of at least two days can be achieved for all 346 references.

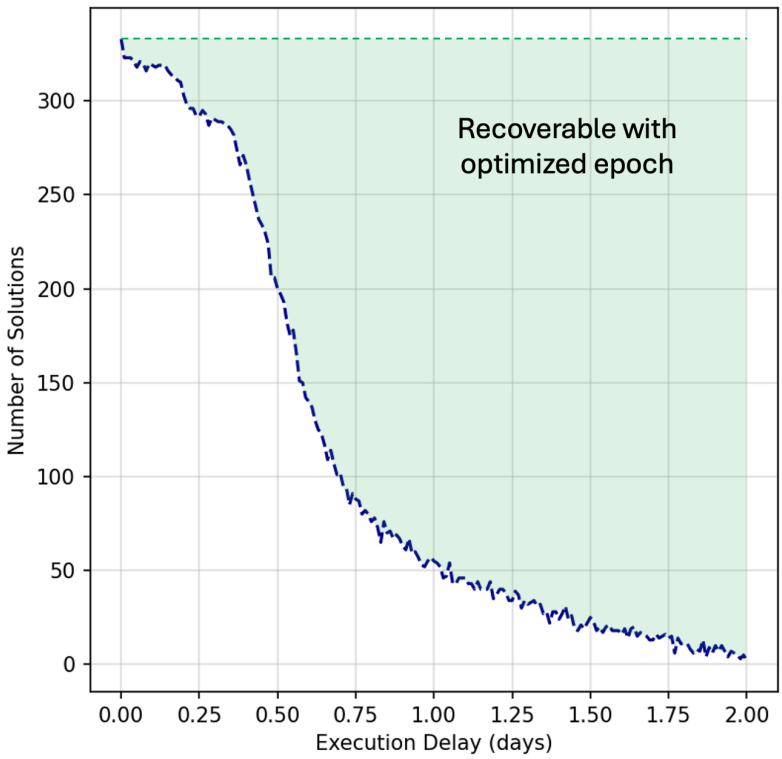

Figure 10: Number of feasible solutions for a given execution delay for fixed NRHO arrival epochs

Figure 11 shows a comparison of impulsive NRHO insertion results, broken down by individual burn magnitude, between a fixed and optimized NRHO insertion epoch for the same baseline reference trajectory. The impact of allowing the insertion epoch to vary can clearly be seen in both the magnitude of Δv required to execute a given recovery as well as the length of execution delays that are enabled by a delayed NRHO arrival. The critical TCA inflection point which occurs at roughly 0.4 days is present in both data sets, however the optimized epoch results display a significantly lower sensitivity to this point. For a fixed NRHO epoch, insertion costs quickly rise as execution delay passes 0.4 days, with an infeasible solution reached near 0.8 days. By optimizing the insertion epoch, execution delays of up to two days (the maximum execution delay analyzed in this work) are enabled while total insertion costs stay below 20 m/s.

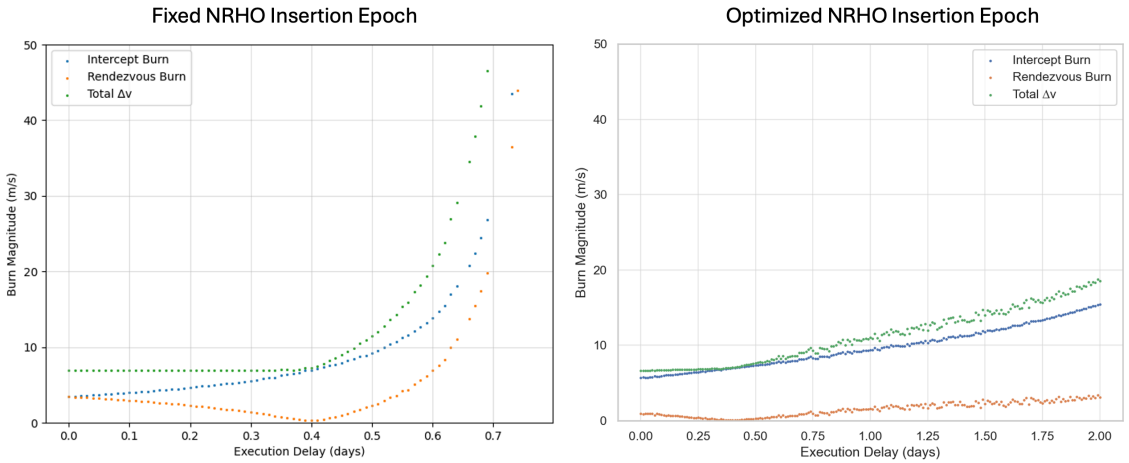

Figure 11: Required Δv as a function of execution delay for a single NRHO insertion. Results for a fixed NRHO insertion epoch are shown on the left while the right shows results where the NRHO insertion epoch was allowed to vary to optimize Δv required. Note the difference in x-axes. Results are broken down by intercept burn magnitude (blue), rendezvous burn magnitude (orange), and total Δv expended (green)

The trends seen in **Figure 11** hold across the entire distribution of results as well as across a single case. **Figure 12** shows the Δv penalty required for an associated execution delay between fixed NRHO insertion epoch cases (left) and optimized insertion epochs (right). It can clearly be seen that optimizing the NRHO insertion epoch results in lower cost solutions across a wider range of execution delays. In particular, optimizing the epoch enables long execution delays for the entire data set, particularly the cheap nominal insertion cases (colored in dark purple). While many fixed epoch solutions require a Δv penalty higher than 40 m/s Δv, few optimized cases require a Δv penalty higher than 20 m/s.

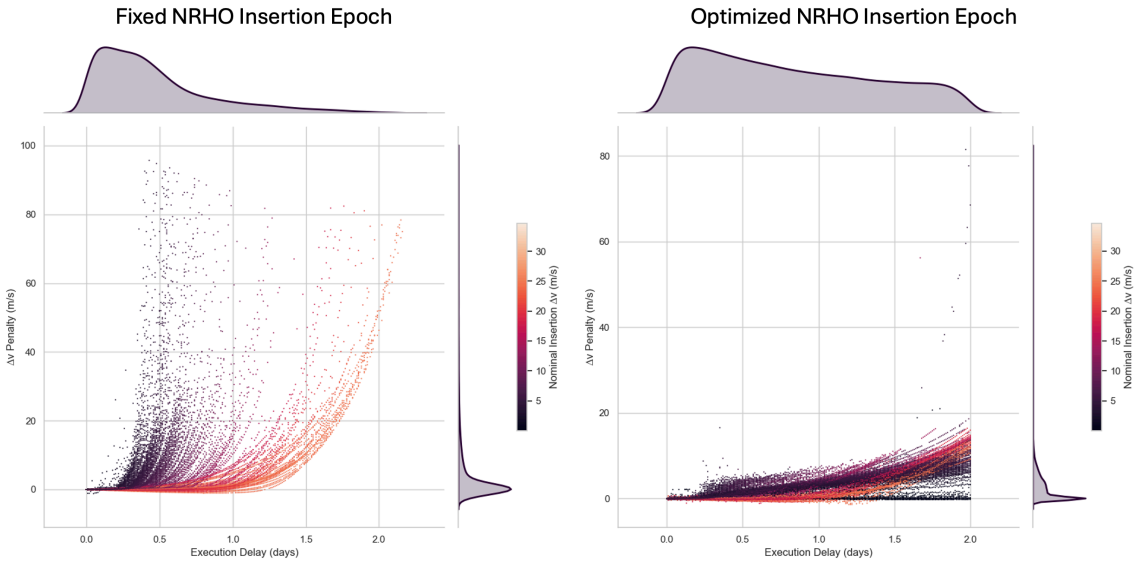

Figure 12: Impulsive NRHO insertion Δv penalty as a function of execution delay, colored by the magnitude of the nominal low-thrust insertion maneuver. Results for a fixed NRHO epoch are shown on the left while results for an optimized NRHO insertion epoch are presented on the right

The broader distribution of potential recovery solutions, and how optimizing the insertion epoch expands this distribution, can very clearly be seen in **Figure 13**. Allowing the insertion epoch to vary uncouples MTE recovery solutions from the duration of the nominal insertion maneuver and enables long execution delays across the entire data set. This optimization also greatly reduces the Δv penalties associated with a given execution delay, resulting in more robust and cheaper recovery solutions. In **Figure 13**, this is seen in the magnitude of the colorbars associated with each plot, where the fixed NRHO insertion epoch cases approach 100 m/s of maximum Δv penalty, while optimization of the insertion epoch reduces this maximum to roughly 20 m/s. Reductions in required Δv penalties for a given execution delay are further illustrated in **Figure 14**. Beyond an execution delay of 0.25 days, the optimization cases uniformly produce lower cost recovery solutions, with results 5x lower than the fixed epoch solutions at an execution delay of two days.

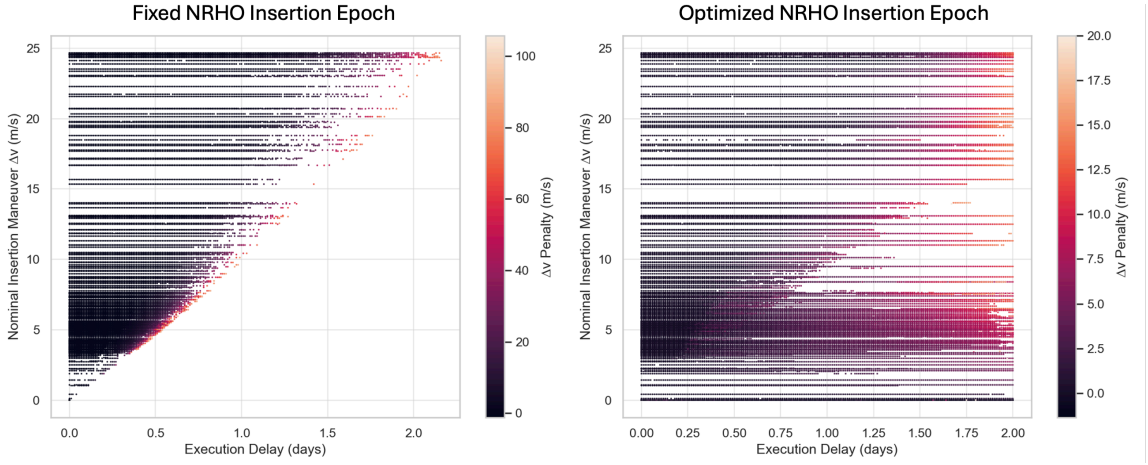

Figure 13: Nominal NRHO insertion maneuver Δv vs execution delay for cases where NRHO insertion epoch was allowed to optimize, colored by Δv penalty. Results for a fixed insertion epoch are presented on the left while results for an optimized insertion epoch are presented on the right

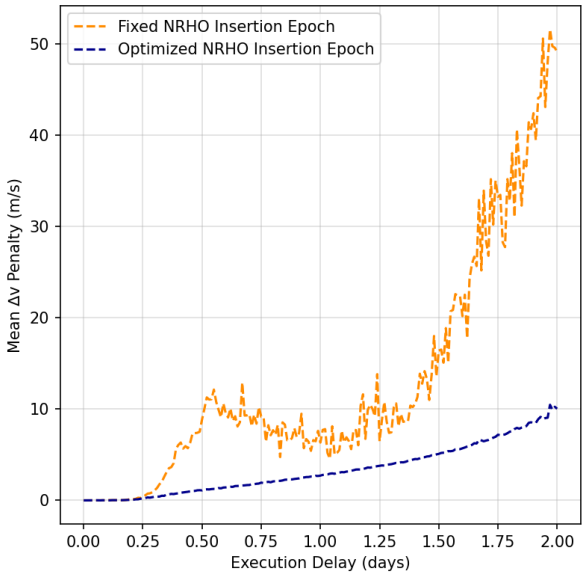

Figure 14: Mean Δv penalty for a given execution delay for fixed NRHO insertion epochs (orange) and optimized NRHO insertion epochs (blue)

The cost of enabling low-cost, long-duration recoveries comes in the form of additional flight time. **Figure 15** shows a histogram of NRHO insertion delays (relative to the nominal NRHO insertion epoch) for the optimized data set. While there are rare instances in which mass-optimal solutions are found that arrive earlier to the NRHO than the reference trajectory, the vast majority of solutions arrive late with an average insertion delay of 1.58 days. As all solutions are constrained to arriving prior to the next perilune passage, the maximum delay encountered is roughly four days.

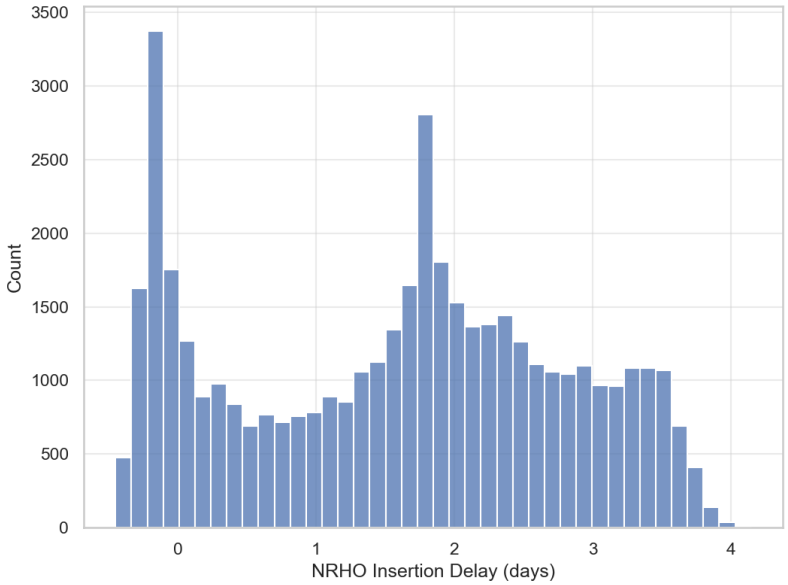

Figure 15: Histogram of NRHO insertion epoch delay relative to the reference trajectory

CONCLUSIONS AND FUTURE WORK

The work presented in this paper represents notional analysis and not a fully mature strategy meant to be implemented during flight. However, these results provide critical insight to engineering and operator teams as to the robustness and resilience of the Lunar Transit trajectory, as designed, to MTEs during NRHO insertion. Previous work[4] has shown that the PPE's 50 kW SEP system can be used to effectively and efficiently recover from MTEs during the Insertion Phase. This paper additionally shows that the onboard high-thrust, chemical RCS can also be used to recover from MTEs. This affords the mission operation team a valuable level of flexibility and redundancy in how MTEs occurring during this critical mission phase can be managed and protected against.

These results suggest that the reference trajectory designs by which Gateway may be delivered to the NRHO are robust against MTEs during final insertion and that sufficient control authority exists to execute this insertion using the RCS. By allowing an insertion delay of up to four days, RCS recovery from an MTE occurring during the NRHO insertion maneuver can be executed for an average of 10.75 m/s impulsive Δv. Additionally, these recoveries provide up to 48 hours of response time during which ground operators can diagnose, troubleshoot, and address the cause of an MTE, verify vehicle health, then plan, upload, and execute a recovery strategy. The solutions presented in this paper will form the basis for continued missed thrust recovery analysis and eventually inform flight rules and operations procedure development for the Lunar Transit of NASA's Gateway.

REFERENCES

[1] D. E. Lee, "White Paper: Gateway Destination Orbit Model: A Continuous 15 Year NRHO Reference Trajectory", *NASA Johnson Space Center*, JSC-E-DAA-TN72594, 2019

[2] M. McGuire, S. McCarty, D. Grebow, T. Pavlak, S. Karn, K. Ponnapalli, D. Davis, K. Hack, et al, "Overview of the Lunar Transfer Trajectory of the Co-Manifested First Elements of NASA's Gateway", *AAS/AIAA Astrodynamics Specialist Conference*, Aug 2021

[3] M. McGuire, S. McCarty, K. Hack, S. Karn, and D. Davis, "Application of Solar Electric Propulsion to the Low Thrust Lunar Transit of the Gateway Power and Propulsion Element", *International Electric Propulsion Conference*, Jun 2024

[4] S. Karn, S. McCarty, M. McGuire, "Recovery from Missed Thrust During Low Thrust Insertion of NASA's Gateway into a Near Rectilinear Halo Orbit", *AAS/AIAA Astrodynamics Specialist Conference*, Aug 2024.

[5] S. Karn, S. McCarty, M. McGuire, "Ballistic Leverage for Conjunction Avoidance During the Lunar Transit Trajectory of NASA's Co-Manifested Vehicle", *AAS/AIAA Astrodynamics Specialist Conference*, Aug 2023

[6] A. Madni, W. Hart, T. Imken, et al, "Missed Thrust Requirements for Psyche Mission" *AIAA Propulsion and Energy Forum*, Aug 2020

[7] Press Release, "Glitch on BepiColumbo, work ongoing to restore spacecraft to full thrust", *European Space Agency*, 2024

[8] C. Ocampo and J. Senet, "The Design and Development of COPERNICUS: A Comprehensive Trajectory Design and Optimization System", *57th International Astronautical Congress*, 2006

[9] P. Gill, E. Wong, et al, "User's Guide for SNOPT Version 7.7: Software for Large-Scale Nonlinear Programming", *University of California San Diego*, Mar 2021

[10] S. McCarty and M. McGuire, "Parallel Monotonic Basin Hopping for Low Thrust Trajectory Optimization", *AAS/AIAA Spaceflight Mechanics Conference*, 2018